Supporting Information for

Plasmonic nanobubbles enhance efficacy and selectivity of chemotherapy against drug-resistant cancer cells

*Ekaterina Y. Lukianova-Hleb, Xiaoyang Ren, Joseph A. Zasadzinski, Xiangwei Wu and Dmitri O. Lapotko**

Methods and Materials

1. Cell culture model. Immortalized normal human oral kerotinocyte NOM 9 cells were cultured in KBM Complete Medium (Cat# CC-3001) from Lonza in a 37°, 5% CO_2 incubator. The OCSCC HN31 GFP stable cell line was built by transfecting the EGFP C1 plasmid into HN31 cells. The selecting marker was G418. The transfected cells were cultured in DMEM High Glucose medium (Cat# 10013 CV) from Mediatech supplemented with MEM Vitamin Solution (Cat# 11120) and MEM NEAA (Cat#11140) both from Gibco and penicillin-streptomycin (Cat# 30002 CT) from Mediatech in the same incubator. For co-culture, the cells were resuspended in KBM media and counted after trypsinization and neutralization. NOM 9 was mixed with HN31 GFP cell in 100:1 ratio and seeded at a density of 20,000 cells/well in 8-well chambered slide (#155409, Nalge Nunc International, Rochester, NY). Cell death (destruction) was measured with Trypan Blue exclusion test in 2-72 hours depending on the cell death mechanism. Therapeutic concentrations *in vitro* for cisplatin, doxorubicin and Doxil were determined using their prescription information.

2. Gold nanoparticles and their targeting. NP-based therapies were realized with 50 nm hollow gold nanoshells synthesized by galvanic replacement of gold on a silver core according to [1]. The advantages of this type of NP are: near-infrared and visible optical excitation, relatively high photothermal efficiency [2], low toxicity and reliable conjugation properties. Maximal optical absorbance of NPs was 820 nm, in the near-infrared (NIR)

window; NIR light is minimally absorbed by all endogenous molecules and by water. 50 nm NPs were conjugated with one of the two antibodies against OCSCC-specific epidermal growth factor receptor, Erbitux (ImClone Systems Inc., Branchburg, NJ) (C225) and Panitumumab (Amgen Inc., Thousand Oaks, CA) by BioAssayWorks LLC (Ijamsville, MD). Conjugated antibodies and small NPs provided efficient targeting through receptor-mediated endocytosis achieved by incubating cells with NP conjugates at 37ºC for variable times (see Fig. S1). As a result of such targeting the NPs were internalized and formed intracellular NP clusters [3-5], likely within endosomes, that determined the main therapeutic effects seen. NPs were characterized by optical spectroscopy and transmission electron microscopy. Uptake of NPs by living cells was visualized with confocal microscopy (LSM-710, Carl Zeiss MicroImaging GmbH, Germany).

3. NP therapies were applied in thermal and mechanical modes by converting the optical energy of excitation laser pulses into heat via the absorption properties of the gold NPs (Fig. 2B). Nano-hyperthermia was achieved through a pulsed (70 ps, 40 Hz) optical exposure of NP-treated cells to low laser fluences at the wavelength of maximal optical absorbance (820 nm). The thermal effect was varied through the accumulated optical dose (J cm^{-2}) that was controlled by exposure time. Use of the short pulses was intended to localize the effect of hyperthermia to single cells, conditions that cannot be achieved with continuous optical excitation due to thermal diffusion. Mechanical therapeutic mode was achieved through the generation of PNBs in individual cells. Increased laser fluence was applied (in order to have sufficient energy to overcome the threshold energy to evaporate water in the local NP environment) by a single NIR laser pulse. The fluence of each laser pulse was measured with a calibrated energy meter and image detector (measured the diameter of laser beam at the cell plane). We used previously developed methods and experimental set-up [6] to image, detect and quantify the thermal and mechanical impacts in individual cells through their optical and

acoustical time-responses detected with probe laser (05-STP-901, CVI Meller Griot, Albuquerque, NM) and XMS310 (Olympus, Waltham, MA) transducer (Fig. 2S). The shape of the time-response was specific and different for a heating-cooling effect without generation of PNB and for generation of PNB, while the duration of the PNB-specific response characterized the PNB lifetime. The maximal diameter of the PNB (which determines the therapeutic effect) is proportional to the PNB lifetime [7,8]. In addition, excellent optical scattering properties of the PNB [2,8] were used for its imaging in cells. The cells were monitored with optical microscopy in bright field, fluorescent and scattering modes. Individual cancer cells were identified through the fluorescence of GFP.

Cell targeting with gold nanoparticles and plasmonic nanobubbles

The size of NP cluster was measured in individual cells through the maximal pixel amplitudes of scattering image as function of the NP conjugate concentration and incubation time (red in Fig. A2A,B). For high concentrations of NPs and short incubation times we found relatively low specificity of NP uptake (Fig. A2A,C). After decreasing the NP concentration by 5 times and increasing the incubation time from 45 min to 24 hours we achieved maximal specificity of NP targeting (Fig. S2B,C). Next, the targeting was studied through the parameters of PNBs generated with single excitation laser pulses in individual cells (Fig. 3A-C). The highest contrast of PNB lifetimes for cancer and normal cells correlated to the optimized NP concentration and incubation time described above (Fig. S2C). PNB lifetime was next studied as a function of the fluence of the excitation laser pulse (Fig. S2D). It was measured through optical and acoustical responses that showed excellent correlation (Fig. S2D,E). Unlike other photo-induced effects in cells (including hyperthermia), PNB generation showed obvious threshold nature. No PNBs were observed in cells at laser fluences below the specific threshold of 15 mJ cm^{-2} (Fig. S2D). Above this threshold the size of PNBs almost linearly increased with the laser fluence, although very differently for cancer and normal cells: PNBs

in cancer cells were several time larger than those in normal cells. This demonstrated good selectivity and tunability of PNBs. Only one or few PNBs were generated in individual cells, apparently around the largest NP clusters. This is very low load compared to published therapeutic loads of NPs employed in other methods [9-12]. Next, NP uptake and PNB lifetime were measured as a function of the targeting antibody, C225 versus Panitumumab (Fig. S2F). Panitumumab showed higher selectivity of NP uptake (Fig. S1C) and larger and more selective PNB clusters compared to C225 (Fig. S2F). Finally, PNB lifetime was measured as the function of the type of gold NP type; previously used hollow gold shells versus solid spheres of similar size, 50 nm. Spheres did not generate any PNBs under near-infrared excitation and their PNB generation threshold in visible region was much higher than for nanoshells. The hollow nanoshells generated PNBs in near-infrared and under the fluence levels below the FDA limit for non-invasive *in vivo* use of pulsed laser radiation [13]. This confirmed the better photothermal efficacy of NSs for cancer treatment. Under identical optical excitation fluences, PNB size (lifetime) depended significantly upon NP cluster state and size: the maximal PNBs were observed for NP clusters while single NPs almost did not generate PNBs (Fig. S2C). This correlated to the size (lifetime) of PNBs in cancer and normal cells (Fig. S2D) and demonstrated that the largest NP clusters, not individual NPs, provided selective generation of PNBs, which generation threshold fluence decreased with the NP cluster size [2, 8] . As a result, we determined that the shell-Panitumumab conjugates formed NP clusters through the EGFR-mediated endocytosis in 24 hours under reduced load of NPs and provided cancer-cell specific generation of PNBs under low optical excitation fluence.

References

1. GH Wu, A Milkhailovsky, HA Khant,C Fu ,W Chiu, JA Zasadzinski, *JACS* **2008**, *130*, 8175.

2. E Lukianova-Hleb, Y Hu, L Latterini, L Tarpani, S Lee, RA Drezek, JH Hafner, DO Lapotko, *ACS Nano*, **2010**, *4*, 2109.

3. DO Lapotko, EY Lukianova-Hleb, AA Oraevsky, *Nanomedicine (Lond),* **2007**, *2*, 241.

4. S Bhattacharyya, R Bhattacharya R, S Curley, MA McNiven, P Mukherjee, *Proc Natl Acad Sci USA*, **2010**, *107*, 14541.

5. Y Nishimura, K Yoshioka, B Bereczky, K Itoh, *Mol Cancer*, **2008**, *7*, 42.

6. DS Wagner, NA Delk, EY Lukianova-Hleb, JH Hafner, MC Farach-Carson, DO Lapotko, *Biomaterials*, **2010**, *31*, 7567.

7. A Vogel, J Noack, G Huttman, G Paltauf, Appl Phys B-Lasers O, **2005**, *81*, 1015.

Cai W, Gao T, Hong H., Sun J. Applications of gold nanoparticles in cancer nanotechnology. Nanotechnology, Science and Applications. 2008;1:17-32.

8. E Lukianova-Hleb, DO Lapotko, *Nano Lett.* **2009**, *9*, 2160.

9. E Boisselier, D Astruc, *Chem. Soc. Rev.* **2009**, *38*, 1759.

10. IH El-Sayed, X Huang, MA El-Sayed, *Nano Lett.* **2005**, *5*, 829.

11. C Loo, A Lowery, N Halas, J West, R Drezek, *Nano Lett* **2005**, *5,* 709.

12. K Sokolov, M Follen, J Aaron, I Pavlova, A Malpica, R Lotan R, R Richards-Kortum, *Cancer Res.* **2003**, *63*, 1999.

13. Laser Institute of America. American national standard for safe use of lasers (ANSI Z136.1–2000). **2000**.

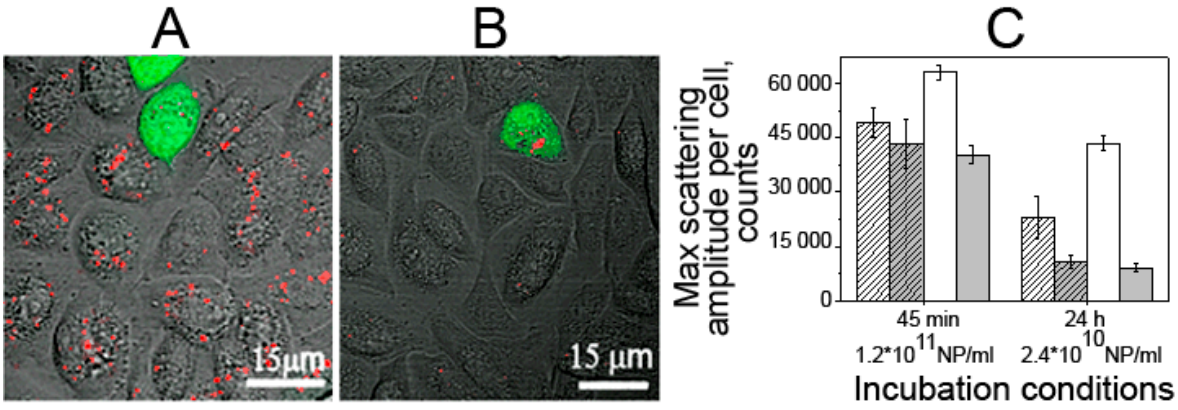

Figure 1S. Overlaid fluorescent, scattering and bright field confocal microscopy images of a co-culture of cancer (green) and normal (colorless) cells with clusters of gold NPs (red). A: NP conjugates were incubated for 45 min at the concentration of $1.2*10^{11}$ NP/ml; B: NP conjugates were incubated for 24 hours at the concentration of $2.4*10^{10}$ NP/ml; C: Diagram for maximal pixel amplitudes (per cell) of the scattering images as metrics of the size of largest NP clusters for the targeting conditions as in A and B for NP conjugates with C225 and Panitumumab (grey bars - cancer cells, white bars - normal cells, shaded bars - C225, clear bars - Panitumumab).

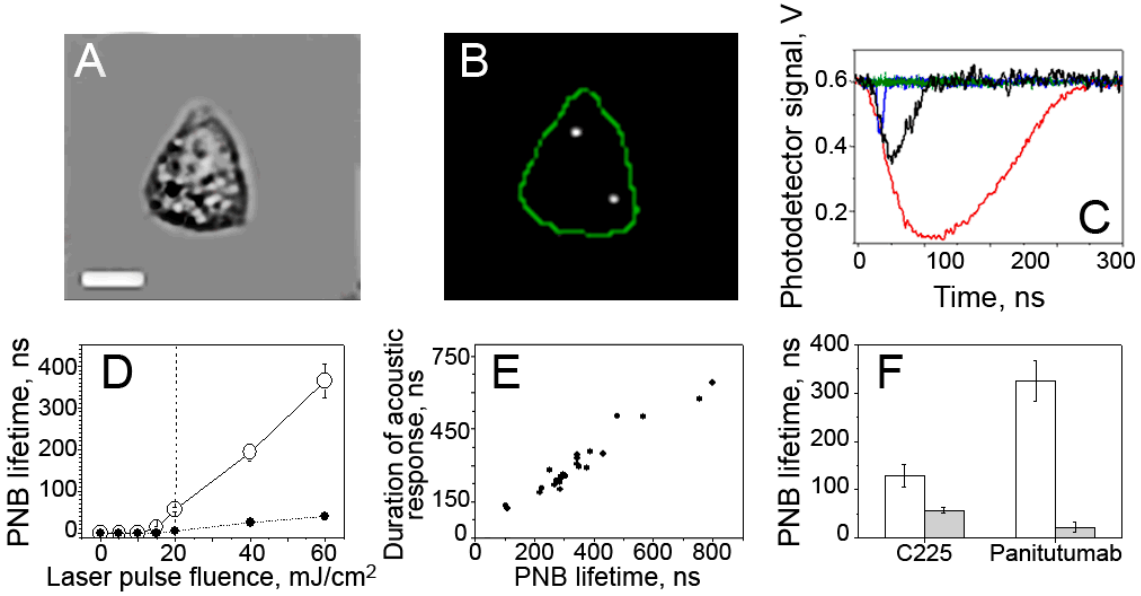

Figure 2S. Plasmonic nanobubbles in NP-treated cells. A: Bright field image of HN31 cancer cell; scale bar is 5 μm; B: optical scattering image of transient plasmonic nanobubbles generated in the same cell with a single laser pulse (70 ps, 820 nm, 40 mJ/cm^2); C: Optical scattering time-responses obtained under the same as above optical excitation conditions for cancer cell (red), normal cell (blue), NP cluster (black) and single NP (green); D: Dependence of the maximal size of PNB (measured as its lifetime through its optical scattering time-response) upon the fluence of excitation (pump) laser pulse (70 ps, 820 nm) for cancer (hollow dots) and normal (solid dots) cells; E: Correlation of acoustical and optical responses from PNBs; F: Dependence of the PNB lifetime in cancer (grey) and normal (white) cells upon the targeting antibody, C225 and Panitumumab (laser fluence 56 mJ/cm^2).

Table S1. Levels of the cell damage and corresponding therapeutic parameters for PNB, hyperthermia and drugs alone and for the combinatorial actions of PNBs and drugs.

Parameter		PNB	Hyper-thermia	Drug			Drug + PNB		
				Cis-platin	Doxo-rubicin	Doxil	Cis-platin	Doxo-rubicin	Doxil
Cell death level, %	Cancer	97±3	91±8	100	97±2	98±1	100	97±2	98±2
	Normal	21±8	63±12	100	98±1	99±1	13±3	33±5	15±2
NP dose, NP/ml		$2.4*10^{10}$	$1.2*10^{11}$		-			$2.4*10^{10}$	
Optical dose, J/cm^2		0.04	24		-		0.025	0.025	0.020
PNB lifetime, ns	Cancer	191±15	-		-		90±10	90±10	65±8
	Normal	28±7					9±5	9±5	11±4
Drug dose, µg/ml		-		20	50	200	2	5	20
Treatment time, s		<1	10^3			$2*10^5$			